5018 *Biochemistry* **2009,** *48,* 5018–5025
DOI: 10.1021/bi900122r

BIOCHEMISTRY
including biophysical chemistry & molecular biology
Article

Nitrosyl Hydride (HNO) as an O_2 Analogue: Long-Lived HNO Adducts of Ferrous Globins[†]

Murugaeson R. Kumar,[‡] Dmitry Pervitsky,[‡] Lan Chen,[‡] Thomas Poulos,[‡,§] Suman Kundu,[∥] Mark S. Hargrove,[∥] Eladio J. Rivera,[⊥] Agustin Diaz,[⊥] Jorge L. Colón,[⊥] and Patrick J. Farmer*[,‡]

[‡]*Department of Chemistry, University of California, Irvine, California 92697,* [§]*Department of Molecular Biology and Biochemistry, University of California, Irvine, California 92697,* [∥]*Department of Biochemistry, Biophysics and Molecular Biology, Iowa State University, Ames, Iowa 50011, and* [⊥]*Department of Chemistry, University of Puerto Rico, Río Piedras, Puerto Rico*

Received January 26, 2009; Revised Manuscript Received April 13, 2009

ABSTRACT: Nitrosyl hydride, HNO or nitroxyl, is the one-electron reduced and protonated form of nitric oxide. HNO is isoelectronic to singlet O_2, and we have previously reported that deoxymyoglobin traps free HNO to form a stable adduct. In this report, we demonstrate that oxygen-binding hemoglobins from human, soy, and clam also trap HNO to form adducts which are stable over a period of weeks. The same species can be formed in higher yields by careful reduction of the ferrous nitrosyl adducts of the proteins. Like the analogous O_2-Fe^{II} adducts, the HNO adducts are diamagnetic, but with a characteristic HNO resonance in ^{1}H NMR at ca. 15 ppm that splits into doublets for $H^{15}NO$ adducts. The ^{1}H and ^{15}N NMR resonances, obtained by HSQC experiments, are shown to differentiate subunits and isoforms of proteins within mixtures. An apparent difference in the reduction rates of the NO adducts of the two subunits of human hemoglobin allows assignment of two distinct nitrosyl hydride peaks by a combination of UV−vis, NMR, and EPR analysis. The two peaks of the HNO−hHb adduct have a persistent 3:1 ratio during trapping reactions, demonstrating a kinetic difference between HNO binding at the two subunits. These results show NMR characterization of ferrous HNO adducts as a unique tool sensitive to structural changes within the oxygen-binding cavity, which may be of use in defining modes of oxygen binding in other heme proteins and enzymes.

Nitrosyl hydride (HNO),[1] the protonated form of nitroxyl anion (NO^-), has distinct physicochemical properties from its congener nitric oxide (NO), much of which has been defined only recently (*1*, *2*). The anionic form is isoelectronic with dioxygen and exists as a triplet, $^3NO^-$, above pH 12; at lower pH, the singlet ^{1}HNO dominates but is susceptible to rapid dimerization, resulting in the formation of N_2O (eq 1) (*3*, *4*). The rate of this dimerization has been reported to be $8 \times 10^6\ M^{-1}\ s^{-1}$ (*5*) and thus severely limits the lifetime and concentration of HNO generated in solution.

$$HNO + HNO \rightarrow N_2O + H_2O \quad (1)$$

HNO is the simplest analogue of alkylnitroso compounds, RNO, long known to bind to ferrous heme proteins (*6*). Mansuy and co-workers were the first to describe the binding of RNO compounds to ferrous globins myoglobin (Mb) and human hemoglobin (hHb) (*7*), as well as to make the analogy of RNO binding to that of dioxygen (*8*). Although quite rare, a number of organometallic HNO complexes of Ir, Os, Re, and Ru have been identified (*9*−*14*), all of which are low-spin d^6 transition metal complexes and diamagnetic (*15*).

$$NO-Mb + e^- + H^+ \rightarrow HNO-Mb \quad (2)$$

$$HNO + Mb-Fe^{II} \rightarrow HNO-Mb \quad (3)$$

In the last several years, we have reported the preparation and characterization of the HNO adduct of myoglobin (HNO−Mb) by electrochemical (*16*) or bulk reduction (*17*) of the ferrous nitrosyl adduct (NO−Mb) (eq 2) and by trapping of free HNO by deoxy myoglobin ($Mb-Fe^{II}$) (eq 3) (*18*). Like the isoelectronic oxy adduct of myoglobin (oxy-Mb), the ferrous nitrosyl hydride adduct (HNO−Mb) is diamagnetic and uniquely characterized by an ^{1}H NMR signal of the N-bound hydride, which is well separated from other protein resonances at ca. 15 ppm. This unique resonance allowed more detailed structural characterization of the heme pocket of HNO−Mb by two-dimensional NOE and COSY experiments (*19*).

[†]This research was supported by the National Science Foundation (PJF CHE-0100774) and the National Institutes of Health (PJF 1R21ES016441-01).

*To whom correspondence should be addressed. E-mail: pfarmer@uci.edu. Telephone: (949) 824-6079. Fax: (949) 824-9920.

[1]Abbreviations: Mb, myoglobin; hHb, human hemoglobin; cHb, clam hemoglobin I from *Lucina pectinata*; lgHb, leghemoglobin; MSHA, methylsulfonylhydroxylamic acid; PA, Piloty's acid; NO, nitric oxide; HNO, nitrosyl hydride; NO^-, nitroxyl anion; DTDP, 4,4′-dimethyl-1,1′-trimethylene-2,2′-dipyridinium; Zn−Hg, zinc−mercury; NMR, nuclear magnetic resonance; HSQC, heteronuclear single-quantum coherence; EPR, electron paramagnetic resonance; UV−vis, ultraviolet−visible spectroscopy.

 Published on Web 04/15/2009

Scheme 1

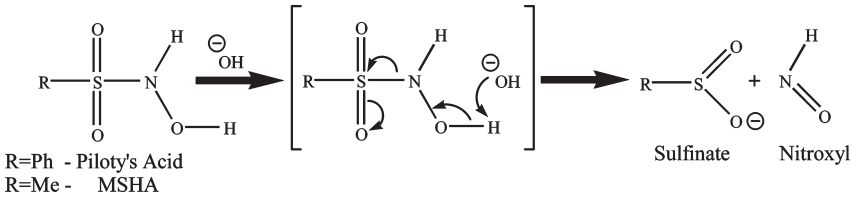

Several routes to HNO−metal complexes have been reported (*15*), but until now, only deoxymyoglobin (Mb−Fe^{II}) has been shown to directly trap free HNO in solution to form an identifiable HNO complex. Because of its limited lifetime, free HNO must be produced in situ from the decomposition of precursors like methylsulfonylhydroxylamic acid (MSHA) or Piloty's acid (PS) (Scheme 1) (*20*). Using such reagents, the trapping of HNO by deoxy-Mb can be observed in time course ^{1}H NMR spectra by the formation of the diamagnetic HNO−Mb, or in UV−vis spectra by the loss of the deoxy-Mb Soret peak (*18*). The maximum HNO−Mb yield obtained by this method is ca. 80%, apparently due to competitive side reactions and further reactivity of Mb−HNO (*21*).

In this report, we demonstrate the ability of other oxygen-binding globins to trap free HNO to form long-lived HNO adducts; examples include recombinant and native isoforms of leghemoglobin (lgHb) (*22*), hemoglobin I isolated from the invertebrate clam *Lucina pectinata* (cHb) (*23*), and human hemoglobin (hHb) (*24*). These HNO adducts can also be generated by careful reduction of the corresponding NO adduct and are characterized by absorbance and ^{1}H NMR spectra, as well as ^{1}H−^{1}H NOESY and ^{1}H−^{15}N HSQC methods. The unique ^{1}H NMR hydride resonance serves as a sensitive indicator of structural changes within the heme pocket, distinguishing subunits and isoforms in protein mixtures.

MATERIALS AND METHODS

General. The HNO precursor phenylsulfonylhydroxylamic acid [Piloty's acid (PA)] was purchased from Cayman Chemicals and recrystallized before use; the precursor methylsulfonylhydroxylamic acid (MSHA) was synthesized and recrystallized by a literature procedure (*25*). ^{15}N-labeled sodium nitrite (98.16% ^{15}N) was purchased from Promy Chemicals. All other chemicals were purchased from Aldrich at 98% purity or better and used as received unless otherwise specified. Water was purified to a specified resistance of 18 MΩ cm in a Barnstead nanopure water purification system before the addition of buffer salts.

Horse skeletal muscle myoglobin (95−100%) and lyophilized human hemoglobin were purchased from Sigma-Aldrich and were used as received. Leghemoglobin (lgHb) was expressed and purified as described previously (*26*). A mixture of leghemoglobin isoforms isolated from soybeans was obtained from Fraser Bergeson and purified using size exclusion chromatography (*27*). Hemoglobin I (cHb) from *L. pectinata* was isolated and purified using size exclusion and ion exchange chromatography (*23*). All manipulations of ferrous proteins were conducted inside an anaerobic glovebox. Purification of proteins was carried out on pre-equilibrated Sephadex G-25 columns in 50 mM phosphate buffer at pH 7 or 9.4.

Absorption spectra for kinetic experiments were recorded with a Hewlett-Packard 8453 diode array spectrophotometer, or for reductive titrations on an Ocean Optics USB 2000 spectrometer in an anaerobic glovebox. X-Band EPR spectra were recorded with a Bruker EMX spectrometer equipped with a standard TE_{102} (ER 4102ST) or a high-sensitivity ER 4119HS resonator. Proton NMR experiments were conducted on Bruker Avance 600 and Varian 800 MHz spectrometers. The spectra were acquired by direct saturation of the residual water peak during the relaxation delay. Chemical shifts were referenced to the residual water peak at 4.8 ppm.

Preparation of Ferrous Heme Proteins. The ferrous states of the heme proteins (lgHb, cHb, and hHb) were prepared by the reduction of the ferric proteins (300 μL, 0.5−0.7 mM) with an ~30-fold excess of sodium dithionite in carbonate buffer at pH 9.4; the resulting ferrous forms were purified on a Sephadex G-25 size exclusion column pre-equilibrated with carbonate buffer at pH 9.4 and then concentrated on a YM-10 membrane filter to give a 0.5−0.7 mM solution.

Reactions of Globins with HNO Precursors and Characterization of HNO Adducts. An anaerobic stock solution of HNO precursor in phosphate buffer (pH 7) was freshly prepared in deionized water before each set of experiments; all manipulations were carried out under a N_2 atmosphere in a glovebox. Samples of HNO adducts of the monomeric globins were prepared anaerobically by addition of 100 μL of an 8.9 mM solution of PA to a ca. 0.5 mM solution of ferrous heme proteins in 50 mM carbonate buffer (pH 9.4). The solution was allowed to stand for 45 min and then purified on a G-25 column using 50 mM phosphate buffer (pH 7). For ^{1}H NMR experiments, the proteins were concentrated on a YM-10 membrane filter to concentrations of 0.5−0.7 mM; typically, 50 μL of D_2O was added to a ca. 450 μL sample of the HNO adduct before measurements.

Similarly, the reaction of 100 μL of 46 mM MSHA with ca. 0.5 mL of 1 mM hHb in 50 mM carbonate buffer (pH 9.4) was followed by time course NMR spectra at 1 h intervals over a day. Afterward, G-25 column filtration was used to remove impurities, and quantification of NO−Hb concentrations was obtained by comparison of doubly integrated EPR spectra of the products with that of an authentic NO−hHb sample. Determined yields of HNO−hHb over six trials ranged from 32 to 48%, per heme content.

Preparation of NO Adducts of Heme Proteins. In a typical procedure, a 200 μL solution of ca. 10 μM ferric heme proteins (lgHb, cHb, and hHb) in 50 mM phosphate buffer (pH 7) was prepared anaerobically and a 10-fold excess of sodium nitrite was added and the mixture allowed to stand for 5 min before the addition of a 30-fold excess of sodium dithionite. The resulting nitrosyl adduct solution was purified by size exclusion chromatography using a Sephadex G-25 column and then concentrated on a YM-10 membrane. Samples of ^{15}NO−ferrous adducts were prepared using 99% $Na^{15}NO_2$.

Reactions of Nitrosyl Globins with Reduced DTDP To Form HNO Adducts. This procedure for chemical reduction

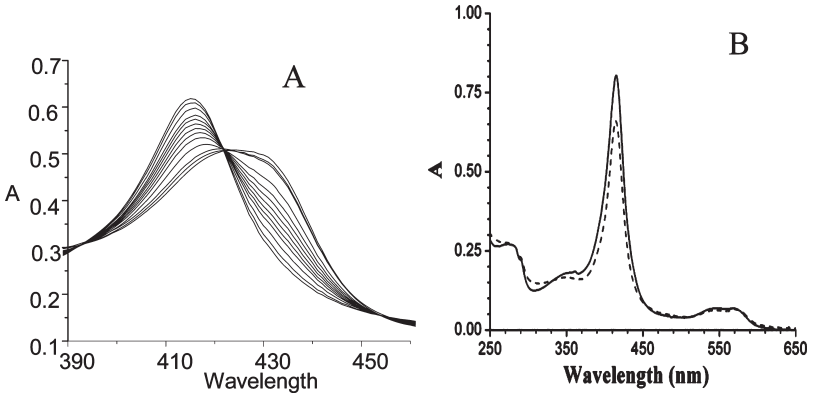

FIGURE 1: (A) Sequential UV−vis spectra of formation of HNO trapping by deoxy-lgHb, forming HNO−lgHb over 30 min during reaction with a 4-fold excess of PA in a 50 mM carbonate buffer (pH 9.4). (B) UV−vis spectra of HNO−lgHb (—) and NO−lgHb (—) at equivalent concentrations, ca. 50 μM in 50 mM phosphate buffer (pH 7).

follows that previously described for HNO−Mb (*28*). A sample of 4,4′-dimethyl-1,1′-trimethylene-2,2′-dipyridinium (DTDP) (0.0024 g, 0.062 mmol) was dissolved in 200 μL of anaerobic 50 mM carbonate buffer (pH 9.4) and reduced with Zn−Hg amalgam (2 mg). Small aliquots (10 μL) of the reduced solution of DTDP were added to NO−hHb (1 mL, 1.5 mM) in an anaerobic glovebox, followed by in situ UV−vis absorbance measurements. A positive shift of the Soret band from 418 to 420 nm is characteristic of HNO adduct formation; a loss of Soret intensity indicates over-reduction, generating deoxy-hHb. The resulting HNO adduct solution was filtered through glass wool, run on a G-25 column using 50 mM phosphate buffer (pH 7), and concentrated for NMR experiments using a YM-10 Centricon as described above.

Quantification of Impurities. As described for HNO−hHb, the percentages of ferrous NO adduct impurities in prepared HNO adduct samples were obtained by comparison of EPR spectra with those of authentic samples, as previously reported for HNO−Mb (*18*, *28*). For example, EPR spectra of NO−cHb and HNO−cHb samples were recorded at the same concentration (normalized by the protein absorbance at 280 nm), and the integrated signals were used to calculate the percentage of NO−cHb impurities in the HNO−cHb sample.

RESULTS AND DISCUSSION

HNO Adducts of Monomeric Globins. The globin protein family is widespread in nature with more than 700 members (*29*); the best known are oxygen binders, e.g., myoglobin and hemoglobin. Leghemoglobin (lgHb) is a small 16 kDa protein responsible for the binding and transport of O_2 to bacteroids in root nodules of legumes; it has an oxygen affinity that is ca. 20 times higher than that of Mb (*30*, *31*). Another monomeric globin, cHb, from the clam *L. pectinata*, binds H_2S in its native role but also forms a stable O_2 adduct; cHb has been widely studied because of a very hydrophobic distal pocket and altered ligand binding affinities (*32*).

Stoichiometric reactions of the deoxy states of lgHb and cHb with HNO donor agent PA at pH 9.4, as illustrated for lgHb in Figure 1, result in absorbance changes similar to those seen during a similar reaction with deoxy-Mb (*18*); the sequential loss of the deoxy state's Soret absorbance gives a direct measure of the reaction with HNO. The reactions are stopped after 45 min by passing the reaction mixtures through a size exclusion column, analogous to the general method developed for generation of HNO−Mb (*21*). After purification, the solutions are stable over weeks when kept anaerobic and in the dark (*28*). These solutions are easily concentrated, and the buffer is exchanged from pH 7 to 9.5 without any appreciable change in the UV−vis or ^{1}H NMR spectra (Table 1). As of yet, there is no evidence of a stable, deprotonated nitroxyl adduct of any protein studied.

Table 1: UV−Vis and ^{1}H NMR Data of Ferrous Globin Adducts

	UV−vis λ_{max} (nm)		^{1}H NMR (ppm)
protein	Fe^{II}−NO	Fe^{II}−HNO	Fe^{II}−HNO
lgHb	414, 548, 571	415, 544, 569	15.0
cHb	420, 541, 568	421, 542, 565	15.53
Mb	421, 548, 580	423, 546, 578	14.80
hHb	418, 543, 580	420, 544 (br)	14.63, 14.80

The formation of HNO adducts is confirmed by ^{1}H NMR spectra of the product solutions which show a characteristic HNO peak between 13 and 16 ppm (Figure 2) (*15*). Also characteristic are peaks below 0 ppm that can be assigned to amino acid residues close to the heme plane; these resonances are shifted upfield due to the porphyrin ring current. The two valine methyl groups in HNO−Mb are seen as two distinct peaks at −0.88 and −2.63 ppm; the latter has strong NOE interactions with the nitrosyl hydride peak (*19*). A similar peak for a distal pocket isoleucine is seen at −1.80 ppm for HNO−lgHb; however, cHb has no equivalent alkyl group above the heme, and no resonance is seen in this region. The hydrophobic distal pocket of this HNO−cHb also has the lowest-field hydride absorbance at 15.53 ppm.

As isolated from soybeans, lgHb is obtained as mixtures of isoforms whose expression ratios change over the life of the plant, and which can be identified by HPLC−MS (*33*). A native lgHb mixture was reduced and reacted with PA as with the recombinant form, and the product solution was analyzed by ^{1}H NMR. As seen in Figure 3, the nitrosyl hydride region shows two overlapping peaks while the distal isoleucine resonances are split into three discernible peaks. Gaussian modeling of the isoleucine resonances gives a ratio of 8:2:4 (supplemental). LC−MS of the native lgHb mixture distinguished three isoforms in a ratio of ca. 4:1:1, in rough agreement with the NMR analysis.

HNO Adducts of Human Hemoglobin. Similar reactions of tetrameric human hemoglobin and PA yield solutions containing HNO−hHb species. ^{1}H NMR analysis of these solutions shows

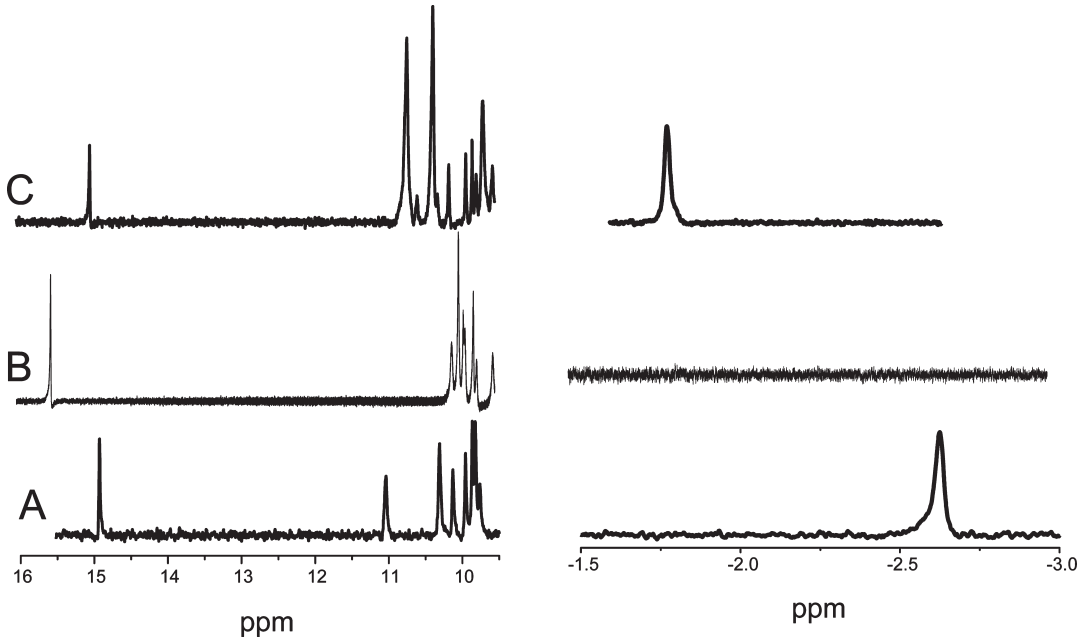

FIGURE 2: ^{1}H NMR spectra of HNO adducts of (A) Mb, (B) cHb, and (C) lgHb generated by reaction of deoxy proteins with PA in carbonate buffers (pH 9.4) and then purified to ~0.5 mM in 50 mM phosphate buffer (pH 7.0).

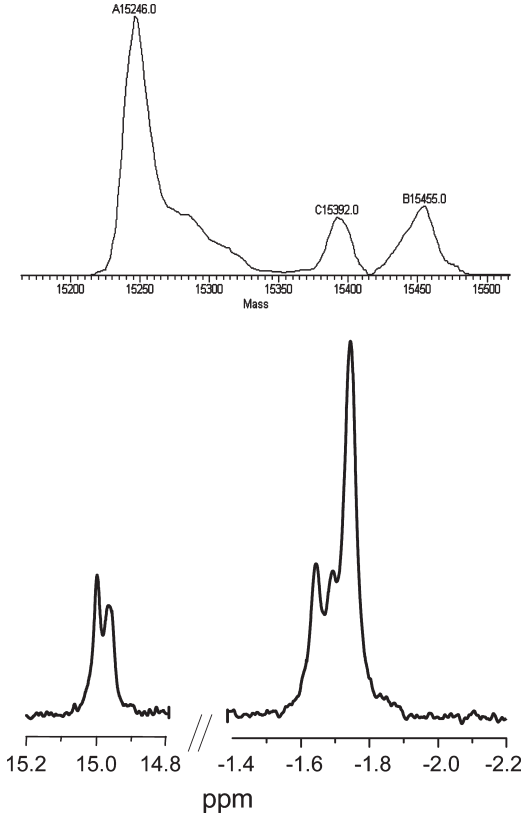

FIGURE 3: Nanospray LC−MS of the wild-type lgHb isoform mixture (top) and ^{1}H NMR spectra (bottom) of HNO−lgHb adducts of this sample (500 μL, 0.7 mM) in 50 mM phosphate buffer (pH 7.0).

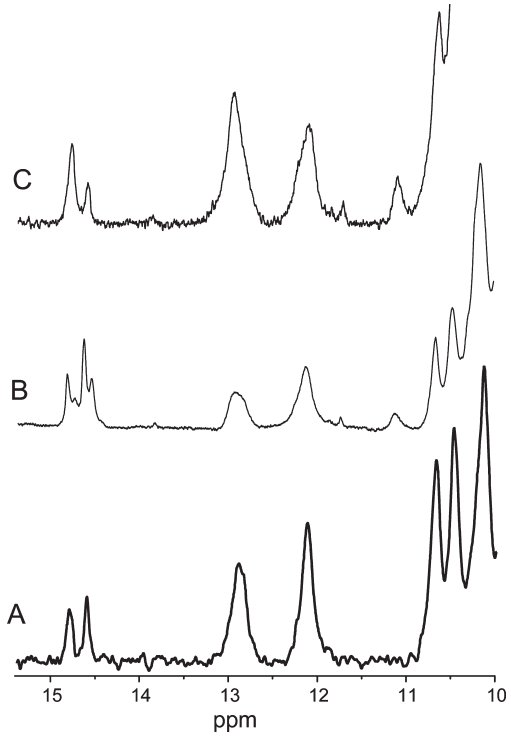

FIGURE 4: ^{1}H NMR of HNO adducts of deoxy-hHb, prepared by different methods. (A) H^{14}NO−hHb prepared by DMDT/Zn reduction of NO−hHb. (B) H^{15}NO−hHb prepared by reduction of ^{15}NO−hHb. (C) H^{14}NO−hHb prepared from deoxy-hHb by trapping of HNO produced by PA decomposition at pH 9.4.

two nitrosyl hydride peaks at 14.63 and 14.80 ppm (Figure 4) in a 3:1 ratio, which can be attributed to HNO adducts of the α and β subunits (vide supra), with resonances assigned to distal pocket valine methyls at −2.18 and −2.23 ppm in a similar ratio. The characteristic doublet splitting of both hydride resonances is also seen for ^{15}N-labeled samples prepared by reduction of ^{15}NO−hHb.

Significantly, two broad resonances are observed at 12.3 and 13.0 ppm (Figure 4), analogous to peaks in ^{1}H NMR spectra of oxy-hHb assigned to protons on Hisα122 and Hisα103 which take part in strong H-bonds between the subunits (*34*). Changes in these signals have been linked to transitions between tensed and relaxed allosteric states upon the binding of O_2, and similar changes can be observed in time course spectra obtained during HNO trapping using the donor MSHA, which releases HNO

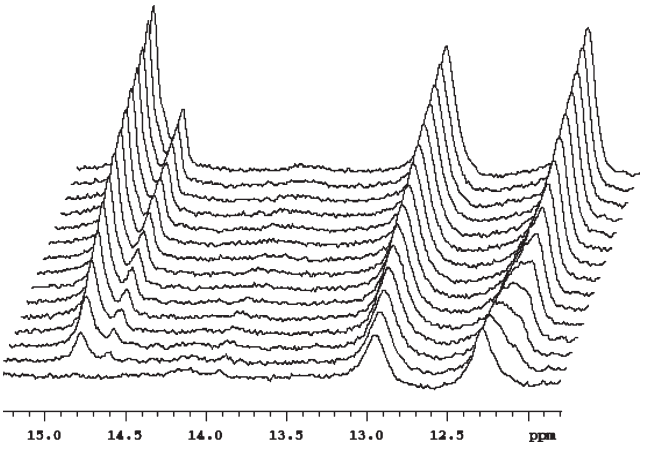

FIGURE 5: ^{1}H NMR time course spectra for the reaction of 40 mM MSHA with 2.0 mM deoxy-hHb in 0.1 M phosphate buffer at pH 9.4 and 25 °C, showing the growth of two nitroxyl peaks at 14.6 and 14.8 ppm and changes in the Hisα122 peak at 12.3 ppm, at 1 h intervals over 16 h.

over hours under these conditions (Figure 5) (*18*, *20*). The shifting of the peak at 12.3 ppm occurs during the initial stages of HNO adduct formation, as might be expected for an allosteric response to ligand binding.

The two nitrosyl hydride peaks have a persistent 3:1 ratio during the MSHA trapping reaction, which was also seen in product mixtures from reactions of deoxy-hHb with PA, demonstrating a kinetic difference in free HNO binding at the two subunits. Similarly, a difference in the reduction rates of the NO adducts of the two subunits has allowed assignment of the nitrosyl hydride peaks by sequential reduction of NO−Hb and concurrent UV−vis, NMR, and EPR analysis, as follows.

A solution of NO−hHb was titrated with reduced DTDP and the reaction monitored by UV−vis spectrophotometry. Sequential samples (A and B) were taken from the solution after titrations had shifted the Soret absorbance from 418 nm of NO−Hb to 419 and 420 nm, as shown in Figure 6. ^{1}H NMR spectra of these samples after concentration displayed the two characteristic HNO−hHb peaks, but that of sample A had a significantly smaller peak at 14.8 ppm as compared to sample B (Figure 6). Comparison of the EPR spectra of these isolated samples revealed significant differences that can be attributed to different subunit contents of ferrous nitrosyl adducts; the spectrum of sample A has enhanced resonances at ca. 3235 and 3330 G, which are characteristic of the ferrous nitrosyl of the α subunit (*35*, *36*). An excess of the nitrosyl adduct in the α subunit implies that of the β subunit has been lost by conversion to the HNO−Fe^{II} state. This logic assigns the ^{1}H NMR peaks at 14.6 and 14.8 ppm to β and α subunits of HNO−Hb, respectively, and peaks at −2.13 and −2.20 ppm to E11 Val peaks of β and α subunits, respectively.

Two-Dimensional NMR Characterization. During initial characterizations of HNO−Mb, ^{1}H−^{1}H NOESY experiments showed a strong cross-peak at −2.67 ppm due to dipolar relaxation of the nitroxyl hydride with a closeby valine methyl group at one side of the heme pocket (*17*); subsequently, more detailed experiments identified some 20 NOEs between the nitrosyl hydride and protein and heme-based signals, which were used to determine the three-dimensional solution structure (*19*). In a similar manner, initial ^{1}H−^{1}H NOESY experiments with HNO−hHb exhibit strong cross-peaks to the distal valine methyl in the two subunits (Figure 7a), suggesting the orientation of the

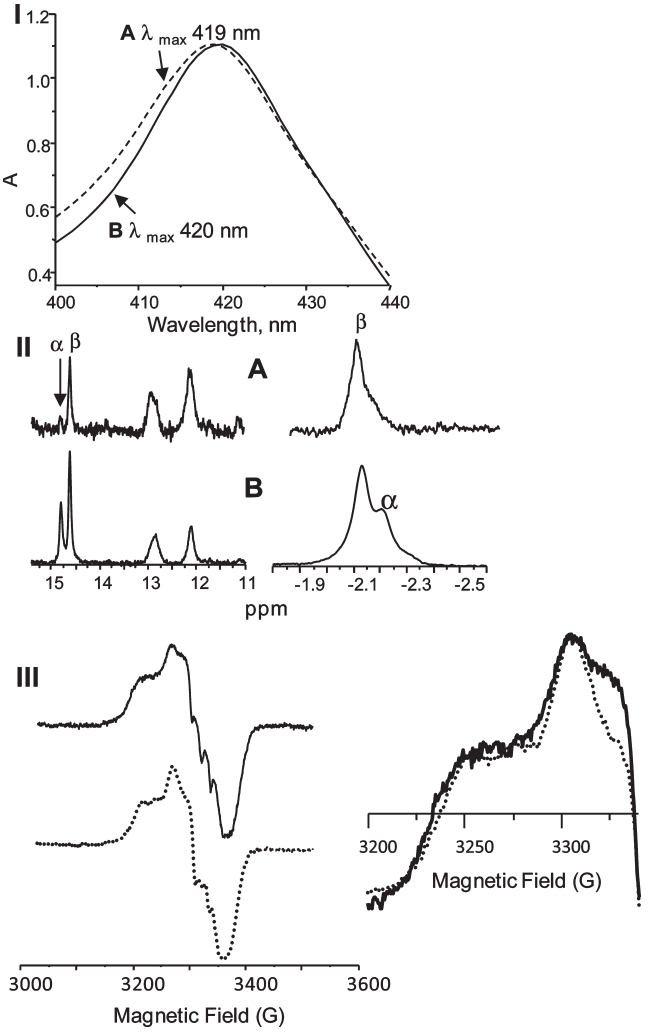

FIGURE 6: (I) Soret band absorbances of partially reduced NO−hHb samples A, with maxima at 419 nm (—), and B, with maxima at 420 nm (—). (II) ^{1}H NMR of HNO−hHb samples A and B. (III) EPR spectra of samples A (—) and B (—).

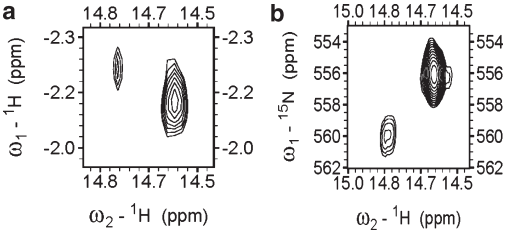

FIGURE 7: (a) ^{1}H−^{1}H NOESY spectrum of HNO−hHb showing cross-peaks between the nitrosyl hydride and distal pocket valine methyl groups. (b) ^{15}N−^{1}H HSQC spectrum of HNO−hHb showing both ^{1}H and ^{15}N chemical shifts for the two subunits.

nitrosyl hydride within the heme pocket is analogous to that of HNO−Mb. ^{1}H−^{15}N HSQC experiments are also useful for HNO adducts as rapid characterizations of both the ^{15}N isomer shifts and J_{NH} coupling values (Figure 7b). The ^{15}N isomer shifts provide an additional unique identifer of a nitrosyl hydride adduct and its electronic environment (Table 2).

Quantification of HNO Adduct Yield. The described reactions generate the HNO adduct in mixtures with other species, the paramagnetic deoxy and nitrosyl adduct species, and accurate quantification is problematic. For the trapping reactions of deoxy globins with HNO precursors, NMR analysis

Table 2: ^{1}H and ^{15}N NMR Chemical Shifts and Coupling Constants of H^{15}NO Adducts of Globins

protein	δ (ppm) ^{1}H	δ (ppm) ^{15}N[a]	J (Hz)
H^{15}NO−Mb	14.87, 14.99	549.1	71.2
H^{15}NO−hHb	14.57, 14.65	560.0	70.39
	14.75, 14.84	556.2	66.37
H^{15}NO−lgHb	14.94, 15.05	553.0	71.19
H^{15}NO−cHb	15.55, 15.44	not available	70.1

[a] From ^{1}H−^{15}N HSQC experiments, referenced to $^{15}NH_4Cl$.

confirms the generation of the diamagnetic HNO adduct, but often smaller paramagnetic peaks due to the NO adduct are seen (*17*). During the early stages of these reactions, the deoxy Soret absorbance is rapidly lost; addition of CO to the headgas over the product mixture produces no change, thus implying minimal deoxy impurity. As given in Table 1, the HNO adduct and NO adducts have absorbance maxima shifted by only 1−3 nm; therefore, EPR analyses of the product solutions are used to quantify the nitrosyl adduct concentration by comparison with authentic samples, and these values are used to estimate the yield of the HNO adduct (Supporting Information). By this analysis, the reaction of PA with deoxy-Mb, ca. 4:1 stoichiometry, gives a yield of 70−80% HNO−Mb (*18*). By comparison, that of HNO−hHb under analogous reactions with PA is ca. 25%, but yields of up to 48% were obtained in slower reactions with the precursor MSHA. The overall yield of the HNO adduct from reactions of PA with other monomeric globins is also low, e.g., 30−40% by EPR calibration of the NO adduct content for cHb.

Reductive titrations of the ferrous nitrosyl adduct samples using the DTDP/Zn−Hg method generate higher-purity samples of the HNO adduct. These titrations are monitored by the typical increase and shift of the Soret absorbance as the HNO adduct is formed; loss of Soret absorbance indicates an over-reduction generating the deoxy species, observable in the absorbance spectra or by CO trapping. This method has been used to generate HNO−Mb at >90% purity (*27*), HNO−hHb in 80% yield, and other globins in an estimated range of 60−90%.

Kinetics of HNO Trapping. The rates of the trapping reactions of ferrous globins were obtained by measuring loss of the ferrous Soret absorbance in sequential UV−vis absorbance spectra taken during reactions with PA over ca. 500 s, as shown in Figure 1 for lgHb. As the generation of free HNO by PA is rate-limiting, the rate constants are modeled with a kinetic simulation program (*37*) utilizing a reaction sequence analogous to that previously reported for Mb (*18*). This sequence includes the release of HNO from PA (eq 4), its dimerization (eq 5), and its trapping by the ferrous globin to form the HNO adduct (eq 6).

$$PhSO_2NHOH + OH^- \rightarrow HNO + PhSO_2^- + H_2O \quad (4)$$

$$HNO + HNO \rightarrow N_2O + H_2O \quad (5)$$

$$cHb{-}Fe^{II} + HNO \rightarrow HNO{-}cHb \quad (6)$$

$$HNO{-}cHb + HNO \rightarrow NO{-}cHb \quad (7)$$

The bimolecular rate constants for HNO trapping resulting from this analysis are on the order of 10^5 M^{-1} s^{-1} for all the monomeric globins (Table 3). For tetrameric hHb, the loss of the deoxy absorbance during HNO trapping reactions is multiphasic over the same period, likely due to allosteric interactions between subunits as well as a competing reaction of HNO with the β-Cys93 (*38*); the value given in Table 3 was obtained by comparison of the loss of deoxy Soret absorbance over 50 s in comparison to Mb under conditions of equivalent heme and PA concentrations (Supporting Information).

Table 3: Initial Rate Constants of Trapping of HNO by Ferrous Globins

protein	rate constant k (M^{-1} s^{-1})
lgHb[a]	1.2×10^5
cHb[a]	9.0×10^5
hHb[b]	ca. 2.0×10^5
Mb[c]	2.2×10^5

[a] As determined by simulations using over 500 s. [b] Over 50 s. [c] From ref *39*.

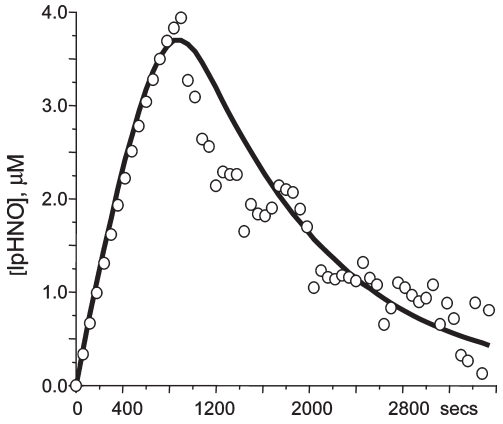

FIGURE 8: HNO binding kinetics. Experimental (○) and calculated (—) concentration profile of HNO−cHb obtained using Soret absorbance changes at 421 nm during the reaction of deoxy-cHb (5 μM) with PA (25 μM) in carbonate buffer (pH 9.4).

A key factor limiting HNO adduct yield in trapping reactions is a subsequent reactivity of the adduct with free HNO (eq 7), previously described for HNO−Mb (*18*, *39*). As a comparison, a more complete modeling was performed for the reaction of cHb and PA over 1 h (Figure 8), using the transient changes at the Soret absorbance of HNO−cHb at 421 nm. Multiple iterations were performed using fixed rate constants for PA decomposition (eq 4) and HNO dimerization (eq 5) until experimental and calculated concentration profiles gave an acceptable match. EPR quantification of the NO−cHb content of the final reaction mixture (Supporting Information) at ca. 80% is in good agreement with the calculated speciation of 85% by the kinetic analysis. The modeled bimolecular rate constant of eq 7 for cHb, at 7×10^4 M^{-1} s^{-1}, is considerably faster than that determined for Mb, at 4×10^3 M^{-1} s^{-1} (*39*), which may explain the lower yield of HNO−cHb obtained under equivalent reaction conditions.

CONCLUSION

This work demonstrates that several oxygen-binding globins react with free HNO in solution to form long-lived HNO adducts and that such adducts can be alternatively formed by careful reduction of the ferrous NO adducts of these proteins. The HNO adducts are diamagnetic and have a unique ^{1}H NMR HNO

hydride signal well away from those of other protein residues. The location of nitrosyl hydride peaks is sensitive to the protein environment and thus differentiates subunits and isoforms within protein mixtures. More broadly, these diamagnetic Fe^{II}−HNO adducts may be of value as models of ferrous oxy complexes and allow characterizations of structural changes accompanying oxygen binding and activation in similar proteins.

ACKNOWLEDGMENT

Electrospray LC−MS was performed by the UCI Center for Virus Research Mass Spec Facility. We also thank Fraser Bergeson for the generous donation of the native lgHb isoform mixture.

SUPPORTING INFORMATION AVAILABLE

Descriptions of peak fitting for isoforms of native legHb mixtures, time course UV−vis spectra during the formation of HNO−hHb, EPR characterization of ferrous NO adduct impurities in HNO adduct samples, and data for initial rate analysis of HNO trapping by deoxy-Mb and hHb. This material is available free of charge via the Internet at http://pubs.acs.org.

REFERENCES

1. Fukuto, J. M., Bartberger, M. D., Dutton, A. S., Paolocci, N., Wink, D. A., and Houk, K. N. (2005) The Physiological Chemistry and Biological Activity of Nitroxyl (HNO): The Neglected, Misunderstood, and Enigmatic Nitrogen Oxide. *Chem. Res. Toxicol. 18*, 790–801.
2. Fukuto, J. M., Switzer, C. H., Miranda, K. M., and Wink, D. A. (2005) Nitroxyl (HNO): Chemistry, biochemistry, and pharmacology. *Annu. Rev. Pharmacol. Toxicol. 45*, 335–355.
3. Shafirovich, V., and Lymar, S. V. (2003) Spin-forbidden deprotonation of aqueous nitroxyl (HNO). *J. Am. Chem. Soc. 125*, 6547–6552.
4. Lymar, S. V., Shafirovich, V., and Poskrebyshev, G. A. (2005) One-electron reduction of aqueous nitric oxide: A mechanistic revision. *Inorg. Chem. 44*, 5212–5221.
5. Shafirovich, V., and Lymar, S. V. (2002) Nitroxyl and its anion in aqueous solutions: Spin states, protic equilibria, and reactivities toward oxygen and nitric oxide. *Proc. Natl. Acad. Sci. U.S.A. 99*, 7340–7345.
6. (a) Richter-Addo, G. B. (1999) Binding of Organic Nitroso Compounds to Metalloporphyrins. *Acc. Chem. Res. 32*, 529–536. (b) Lee, J., Chen, L., West, A. H., and Richter-Addo, G. B. (2002) Interactions of Organic Nitroso Compounds with Metals. *Chem. Rev. 102*, 1019–1065.
7. (a) Mansuy, D., and Chottard, G. (1977) Nitrosoalkanes as Fe(II) Ligands in the Hemoglobin and Myoglobin Complexes Formed from Nitroalkanes in Reducing Conditions. *Eur. J. Biochem. 76*, 617–623. (b) Mansuy, D., Battioni, P., Chottard, J. C., and Lange, M. (1977) Nitrosoalkanes as new ligands of iron(II) porphyrins and hemoproteins. *J. Am. Chem. Soc. 99*, 6441–6443.
8. Mansuy, D., Battioni, P., Chottard, J. C., Riche, C., and Chiaroni, A. (1983) Nitrosoalkane complexes of iron-porphyrins: Analogy between the bonding properties of nitrosoalkanes and dioxygen. *J. Am. Chem. Soc. 105*, 455–463.
9. Melenkivitz, R., and Hillhouse, G. L. (2002) Synthesis, structure, and reactions of a nitroxyl complex of iridium(III), cis,trans-$IrHCl_2$(NH═O)$(PPh_3)_2$. *Chem. Commun.,* 660–661.
10. Southern, J. S., Green, M. T., Hillhouse, G. L., Guzei, I. A., and Rheingold, A. L. (2001) Chemistry of coordinated nitroxyl. Reagent-specific protonations of trans-$Re(CO)_2(NO)(PR_3)_2$ (R = Ph, Cy) that give the neutral nitroxyl complexes cis,trans-$ReCl(CO)_2$(NH═O)$(PR_3)_2$ or the cationic hydride complex [trans,trans-$ReH(CO)_2(NO)(PPh_3)_2^+$][$SO_3CF_3^-$]. *Inorg. Chem. 40*, 6039–6046.
11. Melenkivitz, R., Southern, J. S., Hillhouse, G. L., Concolino, T. E., Liable-Sands, L. M., and Rheingold, A. L. (2002) A new route to coordination complexes of nitroxyl (HN═O) via insertion reactions of nitrosonium triflate with transition-metal hydrides. *J. Am. Chem. Soc. 124*, 12068–12069.
12. Sellmann, D., Gottschalk-Gaudig, T., Haussinger, D., Heinemann, F. W., and Hess, B. A. (2001) [Ru(HNO)('py(bu)S4')], the first HNO complex resulting from hydride addition to a NO complex ('py-buS4'2- = 2,6-Bis(2-mercapto-3,5-di-tert-butylphenylthio)dime thylpyridine(2−1)). *Chem.—Eur. J. 7*, 2099–2103.
13. (a) Marchenko, A. V., Vedernikov, A. N., Dye, D. F., Pink, M., Zaleski, J. M., and Caulton, K. G. (2002) An electron-excessive nitrosyl complex: Reactivity of a ligand-centered radical leading to coordinated HNO. *Inorg. Chem. 41*, 4087–4089. (b) Marchenko, A. V., Vedernikov, A. N., Dye, D. F., Pink, M., Zaleski, J. M., and Caulton, K. G. (2004) Reactivity of the hydrido/nitrosyl radical $MHCl(NO)(CO)(P^iPr_3)_2$, M = Ru, Os. *Inorg. Chem. 43*, 351–360.
14. Lee, J., and Richter-Addo, G. B. (2004) A nitrosyl hydride complex of a heme model [Ru(ttp)(HNO)(1-MeIm)] (ttp = tetratolylporphyrinato dianion). *J. Inorg. Biochem. 98*, 1247–1250.
15. Farmer, P. J., and Sulc, F. (2005) Coordination chemistry of the HNO ligand with hemes and synthetic coordination complexes. *J. Inorg. Biochem. 99*, 166–184.
16. Bayachou, M., Lin, R., Cho, W., and Farmer, P. J. (1998) Electrochemical Reduction of NO by Myoglobin in Surfactant Film: Characterization and Reactivity of the Nitroxyl (NO-) Adduct. *J. Am. Chem. Soc. 120*, 9888–9893.
17. Lin, R., and Farmer, P. J. (2000) The HNO Adduct of Myoglobin: Synthesis and Characterization. *J. Am. Chem. Soc. 122*, 2393–2394.
18. Sulc, F., Immoos, C. E., Pervitsky, D., and Farmer, P. J. (2004) Efficient Trapping of HNO by Deoxymyoglobin. *J. Am. Chem. Soc. 126*, 1096–1101.
19. Sulc, F., Ma, D., Fleischer, E., Farmer, P. J., and La Mar, G. N. (2003) ^{1}H NMR Structure of the Heme Pocket of HNO-Myoglobin. *J. Biol. Inorg. Chem. 8*, 348–352.
20. King, S. B., and Nagasawa, H. T. (1998) Chemical Approaches Toward the Generation of Nitroxyl (HNO). *Methods Enzymol. 301*, 211–221.
21. Sulc, F. (2006) Nitrosyl hydride adduct of deoxymyoglobin: Structure, reactivity and biological importance of Mb-nitrosyl hydride. Ph. D. Dissertation, University of California, Irvine.
22. Appleby, C. A. (1984) Leghemoglobin and Rhizobim Respiration. *Annu. Rev. Plant Physiol. 35*, 443–478.
23. Navarro, A. M., Maldonado, M., Gonzales-Lagoa, J., López-Mejia, R., Lopez-Garriga, J., and Colón, J. L. (1996) Control of carbon monoxide binding states and dynamics in hemoglobin I of *Lucina pectinata* by nearby aromatic residues. *Inorg. Chim. Acta 243*, 161–166.
24. Park, S. Y., Yokoyama, T., Shibayama, N., Shiro, Y., and Tame, J. R. (2006) 1.25 angstrom resolution crystal structures of human haemoglobin in the oxy, deoxy and carbonmonoxy forms. *J. Mol. Biol. 360*, 690–701.
25. Brink, K., Gombler, W., and Bliefert, C. Z. (1977) Methylsulfonylhydroxylamine. *Anorg. Allg. Chem. 429*, 255–260.
26. Hargrove, M. S., Barry1, J. K., Brucker, E. A., Berry1, M. B., Phillips, G. N.Jr., Olson, J. S., Arredondo-Peter, R., Dean, J. M., Klucas, R. V., and Sarath, G. (1997) Characterization of recombinant soybean leghemoglobin a and apolar distal histidine mutants. *J. Mol. Biol. 266*, 1032–1042.
27. Natera, S. H. A., Guerreiro, N., and Djordjevic, M. A. (2000) Proteome analysis of differentially displayed proteins as a tool for the investigation of symbiosis. *Mol. Plant-Microbe Interact. 13*, 995–1009.
28. Pervitsky, D., Immoos, C., van der Veer, W., and Farmer, P. J. (2007) Photolysis of the HNO Adduct of Myoglobin: Transient Generation of the Aminoxyl Radical. *J. Am. Chem. Soc. 129*, 9590–9591.
29. Kapp, O. H., Moens, L., Vanfleteren, J., Trotman, C. N., Suzuki, T., and Vinogradov, S. N. (1995) Alignment of 700 globin sequences: Extent of amino acid substitution and its correlation with variation in volume. *Protein Sci. 4*, 2179–2190.
30. Appleby, C. A. (1992) The origin and functions of haemoglobin in plants. *Sci. Prog. (St. Albans, U.K.) 76*, 365–398.
31. Atanasov, B. P., Dimitrova, E. A., Kudryatseva, N. N., Zhiznevskaya, G. Y., and Appleby, C. A. (1989) Structure of Ferric Soybean Leghemoglobin a Nicotinate at 2.3 Å Resolution. *Biochim. Biophys. Acta 998*, 80–84.
32. Nguyen, B. D., Zhao, X., Vyas, K., La Mar, G. N., Lile, R. A., Brucker, E. A., Phillips, G. N.Jr., Olson, J. S., and Wittenberg, J. B. (1998) Solution and crystal structures of a sperm whale myoglobin triple mutant that mimics the sulfide-binding hemoglobin from *Lucina pectinata*. *J. Biol. Chem. 273*, 9517–9526.
33. Saalbach, G., Erik, P., and Wienkoop, S. (2002) Characterisation by proteomics of peribacteroid space and peribacteroid membrane preparations from pea (*Pisum sativum*) symbiosomes. *Proteomics 2*, 325–337.

34. Mihailescu, M. R., and Russu, I. M. (2001) A signature of the T→R transition in human hemoglobin. *Proc. Natl. Acad. Sci. U.S.A. 98*, 3773–3777.
35. Yonetani, T., Tsuneshige, A., Zhou, Y., and Chen, X. (1998) Electron Paramagnetic Resonance and Oxygen Binding Studies of α-Nitrosyl Hemoglobin. *J. Biol. Chem. 273*, 20323–20333.
36. Hille, R., Olson, J. S., and Palmer, G. (1979) Spectral transitions of nitrosyl hemes during ligand binding to hemoglobin. *J. Biol. Chem. 254*, 12110–12120.
37. Manka, M. J., Ed. (2001) *REACT for Windows*, version 1.2, Alchemy Software, Wesley Chapel, FL.
38. Doyle, M. P., Mahapatro, S. N., Broene, R. D., and Guy, J. K. (1988) Oxidation and Reduction of Hemoproteins by Trioxodinitrate(II). The Role of Nitrosyl Hydride and Nitrite. *J. Am. Chem. Soc. 110*, 593–599.
39. Pervitsky, D. (2008) Generation and reactivity of HNO adducts of horse skeletal myoglobin and human hemoglobin. Ph.D. Dissertation, University of California, Irvine.